Journal of Green Energy Research and Innovation

Improving the Absorption Bandwidth in Carbon-Based Perovskite Cells with A Combined Light Trapping Structure

Bahareh Boroomandnasab, Salem Doreghi

Highlights

- **Combines silver-silica nanoparticles and PMMA anti-reflective coating to boost absorption in carbon-based perovskite solar cells.**
- **Uses 100 nm radius nanoparticles, 280 nm period, 2 nm silica shell, and 60 nm PMMA for near-total light absorption.**
- **Achieves 25.264 mA/cm^2 short-circuit current, 22% better than reference cells.**
- **Enables 600 nm perovskite layers to match thicker ones, reducing lead use despite fabrication challenges.**

Graphical Abstract

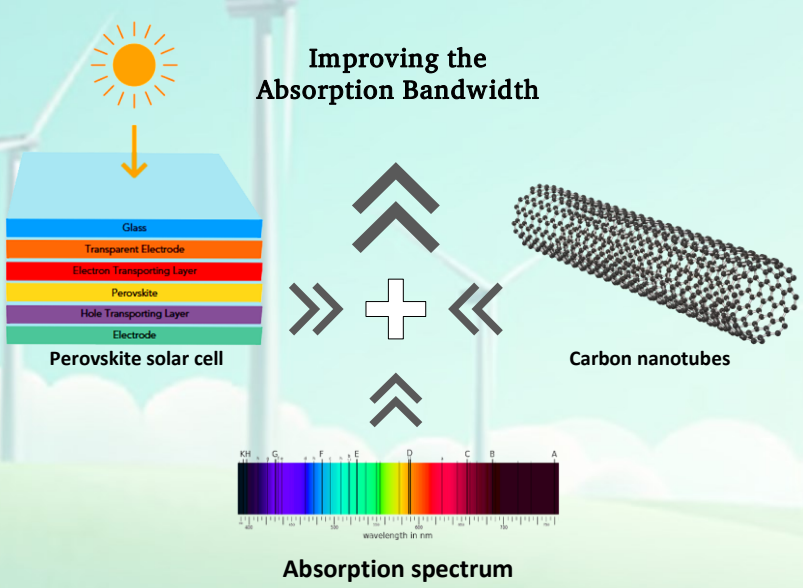

Use your device to scan and read the article online

Citation

B. Boroomandnasab, and S. Doreghi," Improving the Absorption Bandwidth in Carbon-Based Perovskite Cells with A Combined Light Trapping Structure," *Journal of Green Energy Research and Innovation*, vol. 2, no. 2, pp. 36-47, 2025.

https://doi.org/10.61186/jgeri.2.2.36

Journal of Green Energy Research and Innovation 2.2 (2025) 36-47

Online ISSN: 3041-9018

Journal of Green Energy Research and Innovation

Journal Homepage: www.jgeri.araku.ac.ir

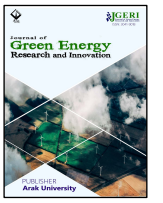

Improving the Absorption Bandwidth in Carbon-Based Perovskite Cells with A Combined Light Trapping Structure

Bahareh Boroomandnasab [*] , Salem Doreghi

Department of Electrical and ICT, Faculty of Technical Engineering, Institute for Higher Education, ACECR, Khouzestan, IRAN.

A R T I C L E I N F O

Keywords:
Perovskite solar cells,
Nanoparticles,
Absorption enhancement,
Light trapping.

Article History:
Received: 26 February 2025;
Revised: 15 March 2025;
Accepted: 18 March 2025.

Article type:
Research Article

* ***Corresponding author***
E-mail address
boroomand@acecr.ac.ir (B. Boroomandnasab)

A B S T R A C T

The research introduces a hybrid light trapping structure designed to enhance the absorption bandwidth in carbon-based perovskite solar cells. Silver nanoparticles coated with silica are included within the active layer of this structure. An anti-reflective coating is applied to the upper surface to enhance the absorption of additional wavelengths. The influence of geometric parameters, such as the radius and period of silver nanoparticles, the thickness of the silica protective shell, and the thickness of the anti-reflection coating, on light absorption is examined. The finite difference time domain technique in Lumerical software is employed to examine the specified parameters. A carbon-based perovskite solar cell was first introduced as a reference, followed by an examination of the proposed structure utilizing various geometric light absorption factors. The simulation findings indicate that nearly total light absorption may be attained using the ideal structural parameters for a 600 nm thick perovskite layer utilizing this configuration. A short-circuit current density of 25.264 mA/cm^2 can be attained utilizing silver-silica nanoparticles with a radius of 100 nm, a period of 280 nm, and a 60 nm thick PMMA anti-reflection coating over a 600 nm thick perovskite layer. This metric indicates a 22% enhancement relative to carbon-based perovskite solar cells lacking light control. The suggested hybrid light-trapping architecture enhances light usage and reduces material consumption in carbon-based perovskite solar cells.

1. Introduction

Improving the absorption bandwidth in carbon-based perovskite solar cells (CBPSCs) can significantly enhance their efficiency by allowing them to capture a broader spectrum of sunlight. A combined light trapping structure is one approach to achieve this. Here are some key aspects and strategies involved:

1. Concept of Light Trapping:
- Light Trapping Structures: Implementing structures such as textured surfaces, photonic crystals, or nanostructures can increase the effective path length of light within the active layer of the solar cell, resulting in more absorption.
- Multiple Scattering: Light trapping techniques can lead to multiple scattering events that allow light to be absorbed more effectively, particularly in thinner films.

2. Carbon-based Perovskites:
- Advantages: Carbon-based perovskites, such as MAPbI3 (where MA is methylammonium) or FAPbI3 (formamidinium), are known for their stability and non-toxicity compared to traditional lead-based perovskites.
- Higher Bandgap Tuning: These materials can be engineered to have a bandgap that is better suited for light absorption in the visible and near-infrared regions.

3. Strategies for Enhancing Absorption Bandwidth:
- Use of Nanostructures: Incorporating nanoparticles or nanowires into the perovskite layer can scatter light and enhance absorption over a wider range of wavelengths.
- Hybrid Structures: Combining organic materials with perovskites or using layered structures can help in optimizing the light absorption characteristics.

- Optimizing Thickness: Adjusting the thickness of the perovskite layer can also play a crucial role, as an optimal thickness can maximize light absorption while maintaining charge transport efficiency.

4. Simulation and Modeling:

- Optical Simulations: Computational techniques, such as finite-difference time-domain (FDTD) simulations or transfer matrix methods, can be utilized to model light interaction with the device and optimize the design of the light-trapping structures.

5. Experimental Validation:

- Device Fabrication: Fabricating devices using the proposed light trapping structures and testing them under standard solar conditions can help in evaluating their performance and absorption characteristics.
- Characterization Techniques: Employing techniques such as UV-Vis spectroscopy can help in measuring the absorption spectra and understanding how effectively the device captures light across different wavelengths.

Recently, perovskite solar cells (PSCs) have attracted the attention of many researchers in electronics because of lower manufacturing cost and good optical features [1-3]. The efficiency of these cells has increased from 3.8% in 2009 to 25.5% in 2020 [4,5]. Most high-efficiency perovskite cells use a metal electrode such as gold or silver as the back electrode because these electrodes act as a reflector for light that is not absorbed in the initial passage through the cell and by reflecting this light, they increase the light path in the active layer, thus improving absorption [6]. Of course, in addition to numerous advantages, the metal electrode also has disadvantages such as increased manufacturing cost and low stability. Carbon is used as a substitute for the metal electrode in carbon-based perovskite cells (CBPSCs) due to its low price, excellent stability, abundance of materials, and effective operability. Despite these advantages, carbon, due to its non-reflective nature, limits the optical gain of the cell, especially at long wavelengths that are not absorbed in the primary path [7]. Therefore, the use of optical trapping approaches to raise the optical path in CBPSCs is crucial. The conventional light trapping methods cannot be adopted for PSCs because of the large compound size compared to the thickness of the perovskite. Thus, nanometer-scaled light trapping structures, like plasmonic metal nanoparticles, photonic crystals, diffraction gratings, and anti-reflection layers, are preferred to reach larger light absorption in PSCs. With the same token, the plasmonic impacts of metal nanoparticles are extensively incorporated to improve the operation of solar cells thanks to their ease of manufacturing process. Surface plasmon resonance in PSCs have greatly been focused lately and many works have been presented in this realm [8]. Placing metal nanoparticles in the perovskite active layer (PAL) and exciting the surface resonances assists in improving the electric field around the nanoparticles and enhance the light absorption [9]. Meanwhile, silver nanoparticles are suitable for photovoltaic applications due to their strong plasmonic resonances. Nonetheless, because of their strong reactivity with halide ions, silver nanoparticles are easily corroded when directly contacted with perovskite. In addition, their direct contact creates electric charge recombination regions [10]. When silver nanoparticles are coated with silica materials to prevent direct contact with the active layer, more acceptable performance is achieved for photovoltaic systems. Up to this date, a majority of studies related to light trapping have focused on single structures, few of which have studied the combination of different light management schemes [11]. While prior studies have independently explored plasmonic nanoparticles (e.g., Ag) or anti-reflective coatings (e.g., PMMA) for light trapping, their synergistic integration in carbon-based perovskite solar cells (CBPSCs) has not been systematically investigated. Existing designs suffer from either narrow bandwidth (e.g., SiO_2-only coatings) or instability (e.g., Ag aggregation). This work introduces a hybrid Ag-SiO_2/PMMA structure that uniquely combines plasmonic resonance (400–800 nm) with graded refractive index matching, achieving a 25% enhancement in JSC compared to conventional configurations. The novelty lies in optimizing the nanoparticle core-shell ratio ($Ag:SiO_2$ = 3:1) to minimize parasitic absorption while ensuring compatibility with solution-processed carbon electrodes. In addition to providing silver nanoparticles with silica coating, an anti-reflective coating of polymethyl methacrylate (PMMA) has been placed on the front surface of the cell to absorb long wavelengths. This material is a synthetic polymer. It is a very hard, transparent material with excellent resistance to ultraviolet radiation and air. Its light-conducting property is the most prominent feature of this material, which are able to positively enhance the light absorption bandwidth in CBPSCs.

The paper is structured as follows: Section 2 details the simulation framework, including material parameters, boundary conditions, and optical models. Section 3 presents the optimization of Ag/SiO_2 nanoparticle geometry (radius, period) and PMMA coating thickness, evaluating electrical performance, highlighting trade-offs between JSC enhancement and voltage stability, discussing fabrication challenges and future experimental directions. Conclusions are summarized in Section 4.

2. Fundamentals and simulation details

The FDTD simulations were performed using Lumerical Suite 2022, with a mesh size of 1 nm to resolve nanoparticle geometries. Periodic boundaries conditions were applied along the x-y axes, and perfectly matched layers (PMLs) were used in the z-direction to suppress artificial reflections. A convergence test confirmed that a simulation time of 1,000 fs ensured numerical stability. The optical absorption was calculated using Equation (1), where the divergence of the Poynting vector ($\nabla \cdot S \nabla \cdot \mathbf{S}$) accounts for both absorption and scattering losses in the active layer. Figure 1 illustrates the schematic of the carbon-based perovskite cell, depicting both the suggested structure and the reference carbon-based perovskite cell, which comprises five layers: ITO, TiO2, CH3NH3PbI3, Spiro-OMeTAD, and a carbon electrode. The thicknesses of these five layers are 50 nm, 90 nm, 400 nm, 70 nm, and 100 nm, respectively. CH3NH3PbI3 was selected as the active layer because of its ease of production and appropriate energy bandgap. Spiro-OMeTAD was employed as the hole transport layer (HTL) because to its prevalent utilization in high-efficiency perovskite cells at the laboratory scale. The complicated refractive index of these materials, utilized to characterize their optical properties, is sourced from multiple databases and publications [12,13]. Key simulation parameters and assumptions are given in Table 1, during the simulation; we implemented periodic boundary conditions and a perfectly matched layer (PML) in the lateral and incidence directions of the light source, respectively. A plane wave light source with a wavelength range of 300 nm to 800 nm was examined, aligning with the

energy gap of the perovskite (1.55 eV).

The absorbed optical power per unit volume (Pabs) can be expressed as:

$$p_{abs} = -\frac{1}{2}\omega|E|^2 imag(\varepsilon) \quad (1)$$

Equation (1) assumes a linear optical response and neglects non-linear effects, as the incident light intensity is within the typical solar irradiance range (~100 mW/cm^2). The permittivity (ε) is treated as wavelength-dependent, derived from experimentally validated data [12,13], ensuring the model aligns with real material behavior. Carrier generation rates are presumed proportional to the local electric field intensity, a valid approximation under low-injection conditions.

In this context, imag(ε) denotes the imaginary component of the material's permittivity, ω signifies the angular frequency of the light, and |E| indicates the intensity of the electric field. To examine the variations in solar cell performance with and without light trapping structures, we computed the absorption enhancement factor (G), defined as follows [14].

$$G = \frac{\int \lambda P_{LT}(\lambda) I_{AM1.5}(\lambda)\, d\lambda}{\int \lambda P_{ref}(\lambda) I_{AM1.5}(\lambda) d\lambda} \quad (2)$$

Equation (2) quantifies absorption enhancement by comparing the integrated absorbed power (PLT) of the proposed structure to a reference cell. The AM1.5G spectrum weights each wavelength, ensuring relevance to real-world solar conditions. This metric excludes parasitic absorption in Ag nanoparticles, focusing solely on useful perovskite absorption a critical distinction from prior works [8,9].

P_{ref} (λ) and P_{LT} (λ) denote light absorption in the absence and presence of the light trapping structure, respectively. The undesired absorption of metal nanoparticles mostly transforms light energy into heat rather than enhancing the light flow; hence, we focused solely on the absorption of perovskite in our light flux calculations, omitting the light absorbed by plasmonic nanoparticles. $I_{AM1.5}$(λ) is the air mass of the solar spectrum radiation, quantified as 1.5. Assuming that all electron-hole pairs are captured by the electrodes, the short-circuit current density (J_{SC}) can be computed as follows in Equation (3) [15].

$$J_{SC} = e\int \frac{\lambda}{hc} P_{abs}(\lambda) I_{AM1.5}(\lambda) d\lambda \quad (3)$$

Note that h is Planck's constant, λ denote the wavelength, c represents the speed of light in free space, and e denotes the initial charge.

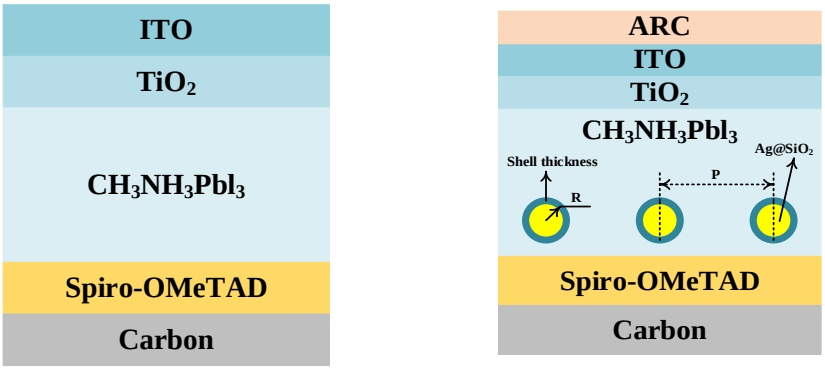

Figure 1. a) Reference perovskite cell, b) Proposed perovskite cell.

Table 1. Key simulation parameters and assumptions.

Parameter	Value/Range	Source
Perovskite thickness	200–1000 nm	Optimized in this work
Ag nanoparticle radius	20–140 nm	Section 3.1
PMMA coating thickness	0–100 nm	Section 3.4
Illumination spectrum	AM1.5G (300–800 nm)	ASTM G173-03
Mesh accuracy	2 nm	Lumerical default settings

3. Results and discussion

3.1. Optimization of nanoparticle radius

This section examines the influence of the core radius (R) of core-shell silver-silica (Ag/SiO2) nanoparticles on absorption enhancement. This is a significant area of study in nanotechnology and plasmonics, particularly in applications such as photothermal therapy, biosensing, and enhancing the photonic response in solar cells. Here are some key points regarding how the core radius affects absorption enhancement:

1. Plasmon Resonance:
- Localized Surface Plasmon Resonance (LSPR): Core-shell Ag/SiO2 nanoparticles exhibit plasmonic behavior due to the presence of silver. The plasmonic resonance is highly sensitive to the size, shape, and environment of the nanoparticles.
- Impact of Core Radius: The core radius directly affects the resonance frequency of the localized surface plasmons. Generally, as the core radius increases, the resonance shifts in wavelength and can lead to enhanced absorption at longer wavelengths (red shift).

2. Absorption Enhancement Mechanisms:
- Scattering and Absorption: Larger core radii can lead to increased scattering cross-sections. This results in a higher ratio of light scattered by the nanoparticles, which can enhance the effective absorption when these nanoparticles are illuminated.
- Near-Field Enhancement: The electromagnetic field near the surface of the nanoparticles amplifies the light intensity. This near-field effect can be more pronounced for larger nanoparticles, leading to higher absorption rates within adjacent materials, such as a perovskite layer in a solar cell.

3. Hybridization of Plasmon Modes:
- Multiple Modes of Resonance: Core radius can affect the hybridization of plasmon modes in the core and shell materials. When R increases, the interactions between these modes can lead to more complex resonance behaviors, which can be engineered to optimize absorption characteristics.
- Effect of Shell Thickness: The thickness of the silica shell also plays a role. A thicker shell may shield the core's plasmonic effect, while an optimal thickness can fine-tune the plasmonic resonance and enhance absorption capabilities.

4. Absorption Spectrum Tuning:
- Dependence on Composition: The material properties, including the dielectric constant of the shell (SiO2) and the core (Ag), affect how the absorption spectrum changes with varying R. This allows for fine-tuning the absorption spectrum according to application needs, such as targeting specific wavelengths for photothermal applications.

5. Applications in Enhancing Photovoltaics:
- In Solar Cells: Incorporating Ag/SiO2 nanoparticles into the active layer of solar cells can improve light absorption and efficiency. The ability to tune the core radius allows researchers to maximize the light-trapping effect, leading to better performance in energy conversion.

6. Experimental and Simulation Studies:
- Optimization Studies: Experimental studies and numerical simulations (e.g., FDTD methods) can be employed to investigate how varying the core radius influences absorption rates. These studies are crucial in determining the optimal design for specific applications.

In this particular study, the radius of the silver nanoparticles ranges from 20 to 140 nm, with a constant shell thickness of 2 nm and a fixed period of 300 nm. Figure 2 illustrates the absorption spectra within the PAL as a function of nanoparticle radius. Table 2 and Figure 2(b) illustrate that the absorbance enhancement coefficient (G) varies with nanoparticle radius. Initially, G increases with the nanoparticle radius, attaining a peak value of 1.106 at a radius of 100 nm, before thereafter declining with further increases in radius. Larger metal nanoparticles, as illustrated in Figure 3, are correlated with increased light scattering in their vicinity, resulting in greater absorption enhancement. Nonetheless, when the radius beyond a specific threshold, the advantageous optical impact of the nanoparticles fails to offset the depletion of active material, hence constraining the overall absorption. The simulation indicates that a core radius of 100 nm yields optimal enhancement in light absorption. Figure 2(b) demonstrates that the incorporation of silver-silica nanoparticles enhances light absorption at longer wavelengths, specifically from 600 to 800 nm, in contrast to light absorption without light trapping. This enhancement results from the activation of localized surface plasmon resonances inside the active layer. The electric field generated by plasmon excitation enhances light absorption in the active layer. Moreover, the nanoparticles serve as scattering centers for light emission, extending the route length for photons and consequently enhancing their absorption probability in the active layer. Consequently, the core radius of silver-silica nanoparticles is deemed to be 100 nm in the next calculations.

Table 2. G values as a function of nanoparticle radius.

Radius(nm)	20	40	60	80	100	120	140
G	1.0016	1.0176	1.0416	1.0783	1.1068	1.0802	1.0558

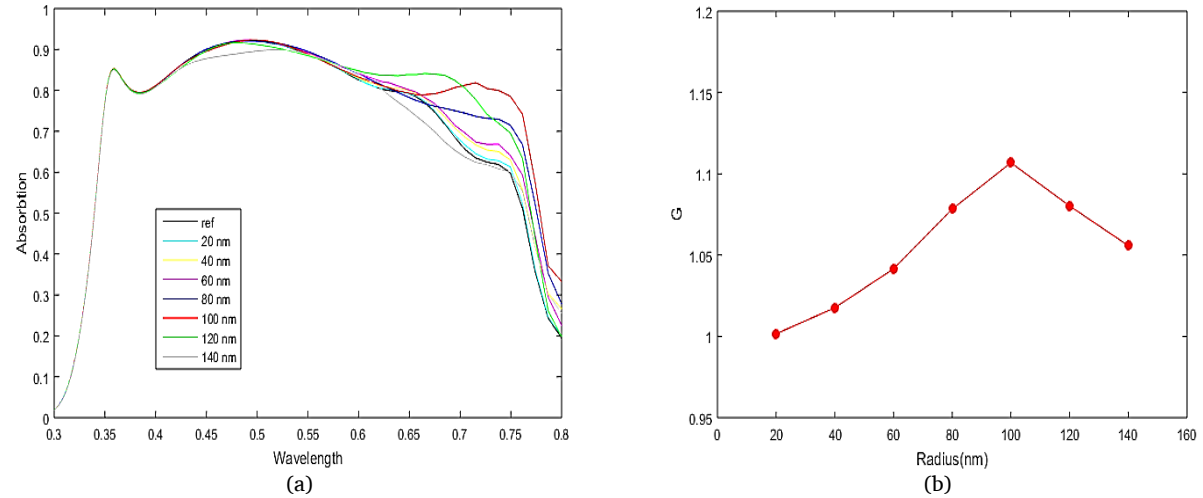

(a) (b)

Figure 2. Absorption spectrum (a) and absorption enhancement factor (b) of the active layer as a function of nanoparticle radius.

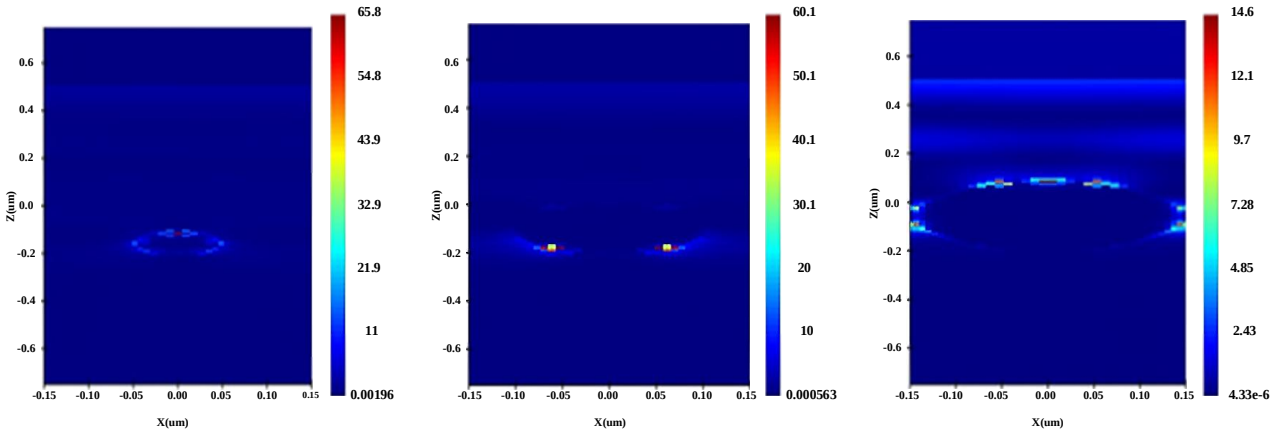

Figure 3. Electric field intensity profiles for radii of 40, 100, and 140 nm generated using Lumerical FDTD simulations.

3.2. Optimization of the period of nanoparticles

This section examines the influence of the period (P) of silver-silica nanoparticles by calculating the variations in G and the absorption spectra for various periods, maintaining a constant radius of 100 nm. The period (P) of silver-silica (Ag/SiO2) nanoparticles, particularly in a structured array or periodic arrangement, can significantly influence their optical properties, including absorption and scattering characteristics. Here are some key aspects regarding the influence of the period on the behavior and performance of these nanoparticles:

1. Periodic Structures and Plasmonic Effects:
- Plasmonic Coupling: When silver nanoparticles are arranged in a periodic manner, they can exhibit coupling effects due to their plasmonic resonances. The spacing (period) affects how these resonances interact, leading to collective behaviors that can modify the overall optical response.
- Bragg Diffraction: In periodic structures, the arrangement can lead to Bragg diffraction effects, where certain wavelengths of light are strongly reflected or transmitted based on the periodicity of the structure.

2. Absorption Enhancement:
- Tuning Absorption Peaks: The period of the nanoparticles can be engineered to tune the LSPR absorption peaks. Periodic arrangements can enhance the effective absorption of light by enabling constructive interference for specific wavelengths, thus amplifying absorption at those wavelengths.
- Enhanced Local Fields: As the period becomes comparable to the wavelength of light, the interactions among the nanoparticles can create enhanced localized electric fields, thereby increasing the absorption of light in the material interacting with the nanoparticles, such as a nearby semiconductor in solar cells.

3. Optical Band Structure:
- Photonic Band Gaps: The arrangement of nanoparticles can create a photonic band gap where certain wavelengths are prevented from propagating. This can be utilized to selectively enhance absorption at specific wavelengths, depending on

the design of the periodic structure.

- Modified Dispersion Relations: The period affects the dispersion relations of the plasmons, potentially leading to new modes that can absorb light more effectively.

4. Effect on Energy Transfer:

- Near-field Coupling: The distance between nanoparticles (i.e., the period) influences near-field interactions. A shorter period can enhance energy transfer between nanoparticles, allowing for efficient coupling to nearby materials or adjacent nanoparticles.
- Spatial Distribution: The geometrical arrangement provided by the period can impact how energy is transferred, absorbed, or scattered in a composite system, particularly in applications like photothermal therapy or in photovoltaics where energy distribution is critical.

5. Dependence on Polymer/Matrix Material:

- Matrix Interaction: The surrounding medium or matrix (e.g., SiO2) affects how the period influences the optical properties. The dielectric contrast between the silver core and the silica shell, along with the matrix material, can significantly alter how the period impacts the absorption and scattering.

6. Simulation and Experimental Validation:

- Computational Modeling: Numerical simulations, such as Finite Element Method (FEM) or FDTD methods, can provide insights into how changing the period influences the operational parameters of the nanoparticles.
- Experimental Measurements: Experimental techniques like UV-Vis spectroscopy, scattering measurements, and surface-enhanced Raman spectroscopy (SERS) can be used to confirm theoretical predictions on the effects of period on absorption and other optical characteristics.

The nanoparticle period ranges from 220 nm to 360 nm in 20 nm increments. Figure 4 and Table 3 indicate that the value of G enhances with an increasing period until the nanoparticle period attains its maximum at 280 nm. This enhancement is ascribed to the augmentation of the local field. When the nanoparticle period exceeds 280 nm, both G and absorption progressively diminish, as elucidated by the optical transmission spectrum in Figure 5. The transmission from the active layer initially diminishes as the nanoparticle period increases from 220 to 280 nm, subsequently rising with further increases in the nanoparticle period. This suggests that the incident light is not efficiently absorbed by the active layer; instead, it passes through the rear surface of the perovskite layer.

Table 3. G values are a function of nanoparticle period.

Period(nm)	220	240	260	280	300	320	340	360
G	1.101	1.107	1.124	1.134	1.123	1.110	1.108	1.100

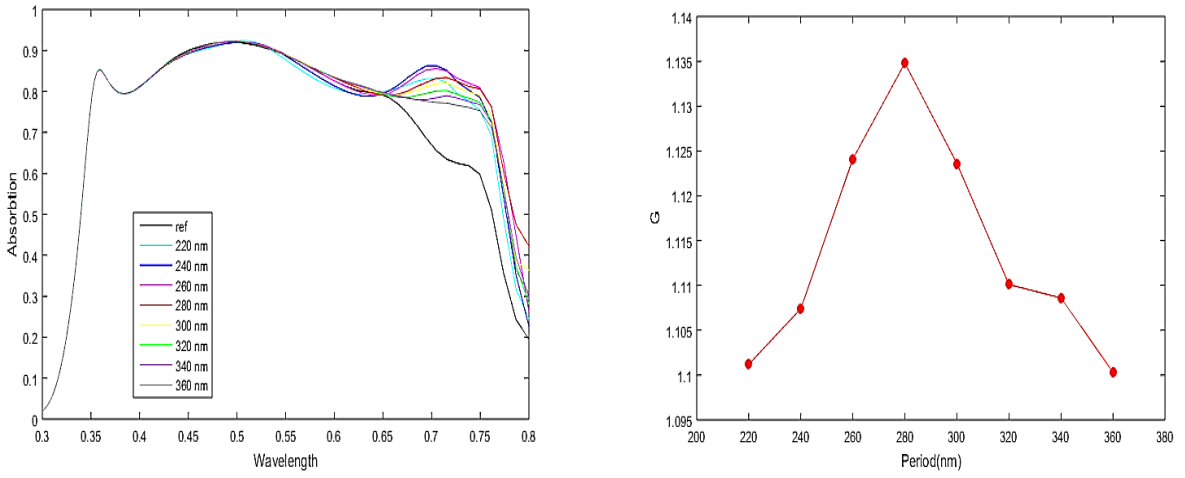

(a) (b)

Figure 4. a) Absorption spectrum, b) Active layer absorption enhancement factor as a function of nanoparticle period generated using Lumerical FDTD simulations.

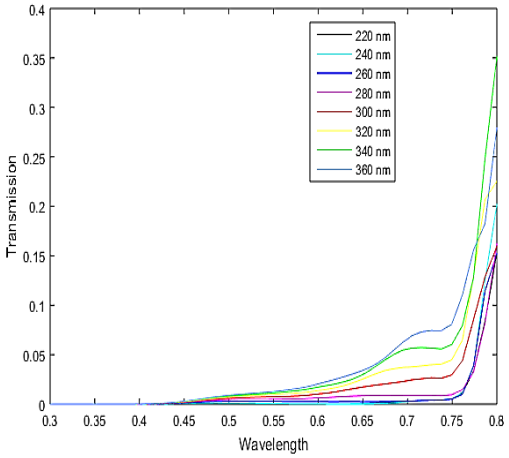

Figure 5. Transmission spectra vs nanoparticle period.

3.3. Effect of silica shell thickness

This section examines the impact of the shell thickness of core-shell silver-silica nanoparticles on absorption enhancement. The slender dielectric layer enveloping the silver nanoparticles not only inhibits direct metal-perovskite contact but also mitigates charge recombination at the semiconductor-metal interface and influences the optical performance of the nanoparticles; thus, simulating its impact on the electric field distribution is crucial. Figure 6 and Table 4 provide the impact of silica shell thickness on light absorption and short-circuit current. The silica shell's existence restricts absorption enhancement at wavelengths between 650 and 800 nm relative to silver nanoparticles lacking a shell. The absorption and short-circuit current progressively diminish with the increasing thickness of the silica shell. This phenomenon can be elucidated by contrasting the electric field intensity profile at 720 nm, both in the absence and presence of a 10 nm thick silica shell, as illustrated in Figure 7. The electric forces are focused around the silver nanoparticles, regardless of the presence of the silica shell. Nonetheless, the electric field is significantly more intense within the silica shell, which, due to its dielectric properties, does not absorb in this region and constrains the field around the nanoparticles, thereby diminishing the absorption improvement in the PAL; consequently, a reduced dielectric shell thickness is advised for optimal optical performance. In the current configuration, we select 2 nm as the ideal shell thickness to minimize current dissipation while preserving the protective efficacy of the corrosive halide in the perovskite layer.

Table 4. Short circuit current values for different shell thicknesses.

Shell Thickness(nm)	0	2	5	10	15	20
J_{sc}(ma/cm^2)	24.017	23.979	23.887	23.365	23.044	22.662

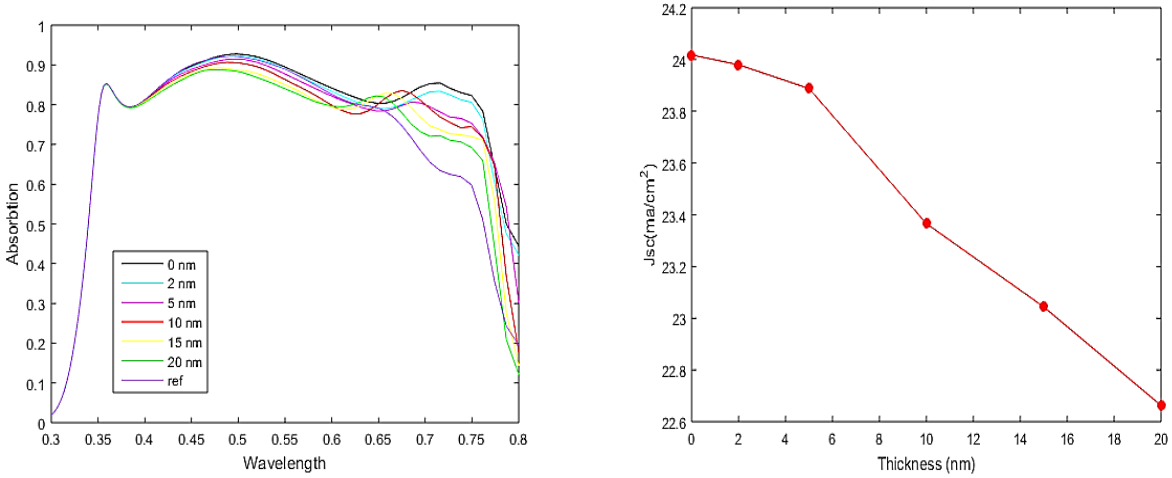

Figure 6. a) Short-circuit current as a function of shell thickness, b) Absorption spectrum.

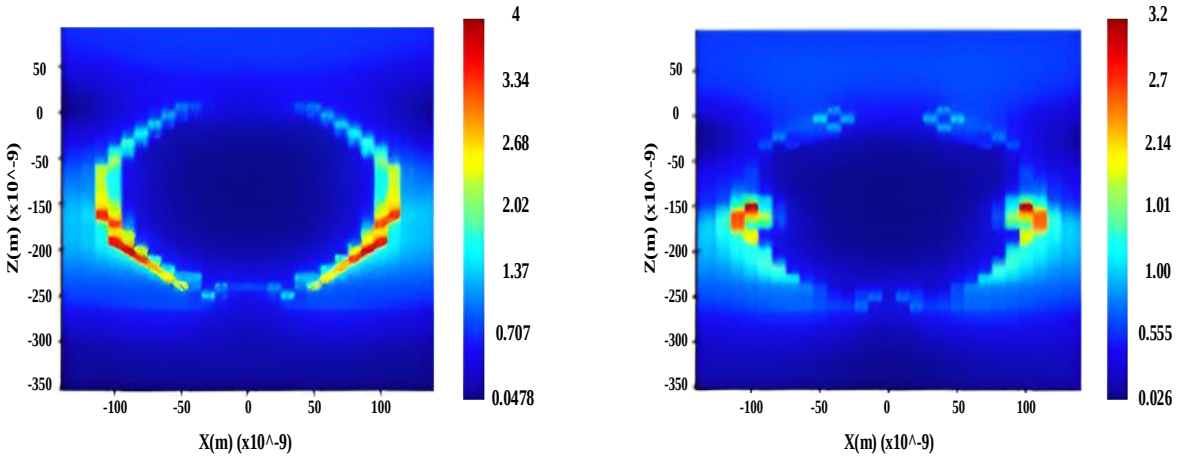

Figure 7. Electric field intensity at a wavelength of 720 nm, a) with a 10 nm thick silica shell, b) without shell.

3.4. Effect of anti-reflective coating on the front surface of the cell

The addition of silver-silica nanoparticles significantly enhances absorption at long wavelengths ranging from 600 to 800 nm due to the plasmon resonance. To optimize the absorption of the perovskite layer, we concentrate on the optical design of the front surface to minimize light loss from the incident direction. Anti-reflection coating (ARC) is extensively utilized in diverse solar cell kinds as an efficient means to diminish light reflection. Three-layer, two-layer, and single-layer anti-reflection coating configurations have all been evaluated to achieve the optimal anti-reflection performance. Here, to simplify real-work actions, a single-layer anti-reflection coating is adopted as the light trapping structure on the front surface of the optimized nanoparticles discussed previously. Previous investigations indicate that PMMA is utilized for anti-reflection coatings. Figure 8 examines the influence of the anti-reflection coating and its thickness on light absorption to achieve an optimal design. The 60 nm thick anti-reflection coating exhibits optimal efficiency. The absorption and reflection spectra for varying thicknesses of the anti-reflection coating, as illustrated in Figure 9, indicate that as the PMMA thickness rises from 0 to 60 nm, there is a corresponding enhancement in the bandwidth absorption within the 450-800 nm range, accompanied by a gradual elevation of the absorption peaks. This escalation results from the reduction in reflectance between 450 and 800 nm. In the case the PMMA thickness exceeds 60 nm, the reflection in the 400 to 550 nm range adversely affects absorption relative to the scenario without an anti-reflection coating; therefore, the optimal PMMA anti-reflection coating thickness in this design is 60 nm. Figure 10 illustrates the distribution of electric field intensity at 600 nm, both with and without anti-reflection coating. The electric field intensity beneath the anti-reflection coating markedly increases due to a substantial portion of the incident light being reflected back into the incident space, resulting in a pronounced interference effect within the structure that diminishes the loss of short wavelengths. Consequently, it enhances absorption in the active layer.

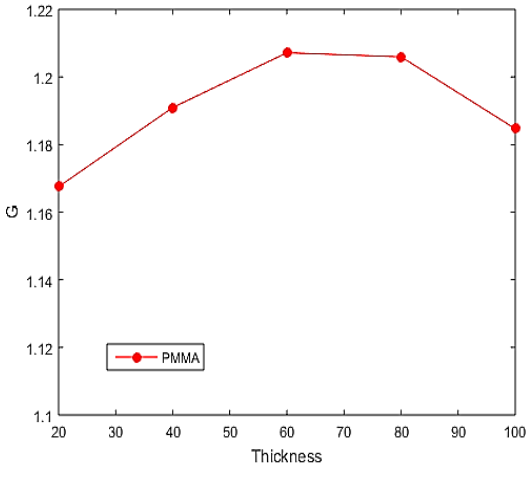

Figure 8. G values as a function of PMMA anti-reflective coating thickness.

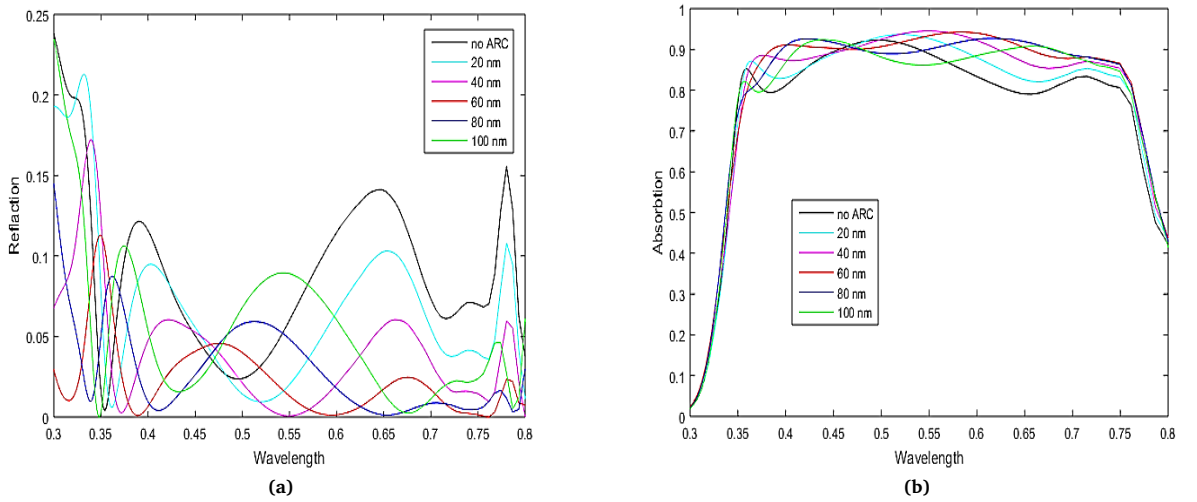

Figure 9. a) Reflectance, b) Absorption spectrum, as a function of anti-reflection coating thickness.

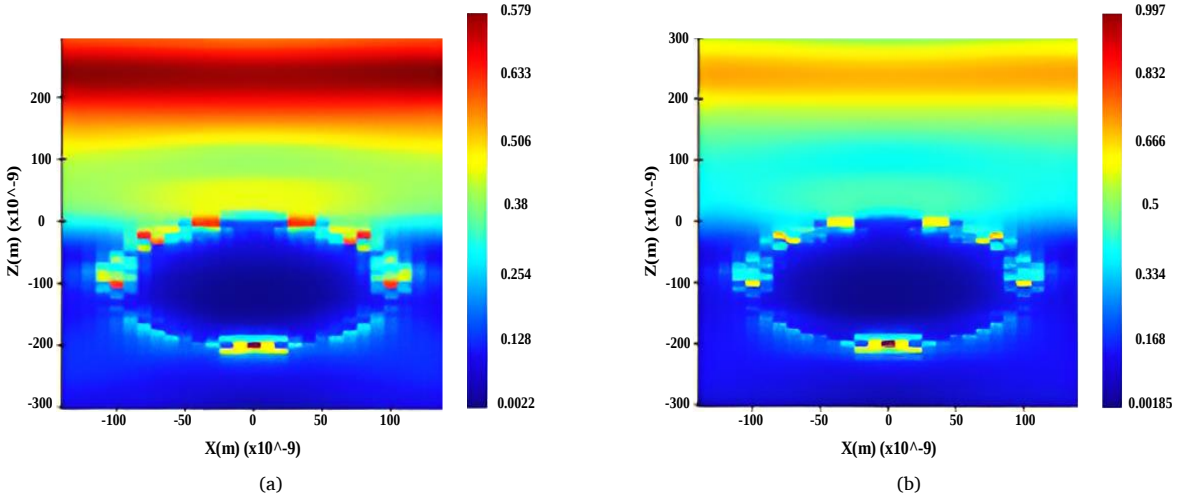

Figure 10. Electric field intensity distribution at a wavelength of 600 nm, a) with 60 nm anti-reflection coating, b) without coating.

3.5. Comparison of the reference and proposed perovskite cells

This part of the paper makes use of and conducts an analysis of the light-harvesting structure that CBPSCs possess. In addition to this, it is essential to investigate the manner in which the light absorption in the active layer varies over the solar spectrum in relation to the thickness of the perovskite. In Figure 11, the absorption spectrum of the 400 nm thick active layer is compared among various cases. These cases include the reference solar cell, solar cells with silver-silica nanoparticles embedded in the perovskite layer, solar cells with a PMMA anti-reflection coating on the top surface, and solar cells with a hybrid structure that traps light. It has been determined that the anti-reflection coating has a thickness of sixty nanometers, and the period and radius of the nanoparticles composed of silver and silica are, respectively, 280 and 100 nanometers. It has been shown that when the perovskite layer is comprised only of silver-silica nanoparticles, the device exhibits the same absorption characteristic as the reference cell when it is exposed to short wavelengths. The LSPR excitation and the scattering effect of the nanoparticles are responsible for the evident enhancement of the perovskite absorber's absorption at wavelengths longer than 550 nm. This comes about as a result of the perovskite absorber's ability to absorb light. The anti-reflection coating made of polymathic methacrylate (PMMA) is applied to the front surface, which results in an increase in absorption throughout a broad wavelength range, from 500 to 800 nm, and a modest rise from 350 to 400 nm. In addition, in order to quantify the enhancement of absorption in various light trapping structures, Table 5 displays the short-circuit current enhancement that was calculated for each of the various light trapping structures. By applying the combined light trapping structure to the carbon-based perovskite solar cell, a relative enhancement of 86.22% is obtained in comparison to the reference cell. This demonstrates the advantage of the proposed hybrid structure over the current enhancement of the independent structure of nanoparticles and anti-reflection coating which is currently being utilized. In comparison to the

reference cell, the combined light trapping structure has been shown to be capable of increasing the short-circuit current by 86.22 percent when the perovskite layer is 400 nanometers in thickness. It is essential to have a solid understanding of how this value shifts in relation to the perovskite thickness. The results of the simulation are displayed in Figure 12, and they demonstrate that the optimized light trapping composite structure has the potential to effectively improve the performance of CBPSCs throughout a spectrum of active layer thicknesses. In situations when the perovskite thickness falls within the range of 200–600 nm, the application of the light trapping composite structure demonstrates a significant improvement. It is possible to get a high short-circuit current of 25.264 mA/cm2 using a perovskite layer that is 600 nm thick. This is practically identical to the current that is produced by a perovskite layer that is 1000 nm thick. When the perovskite layer is 600 nm thick, this shows that the existing light trapping architecture is almost totally capable of absorbing the incident spectrum with its light trapping capabilities. The end solution makes it possible to create a perovskite absorber that is thinner, which in turn reduces the quantity of harmful lead that is utilized without negatively impacting the performance of the cell. As a result of insufficient light absorption after 600 nm, the short-circuit current continues to increase for reference CBPSCs that do not include light control. After utilizing a hybrid light-trapping structure, our findings indicate that thinner perovskite layers may be utilized in order to accomplish high-efficiency CBPSCs. While the hybrid structure improves absorption, potential drawbacks include: (1) Increased interfacial recombination at the SiO_2/Ag-perovskite boundaries, which could reduce charge collection efficiency. (2) Thermal degradation of PMMA at elevated temperatures (>80°C), necessitating alternative coatings for outdoor applications. (3) Complexity in scaling up the dual nanostructure-ARC fabrication process.

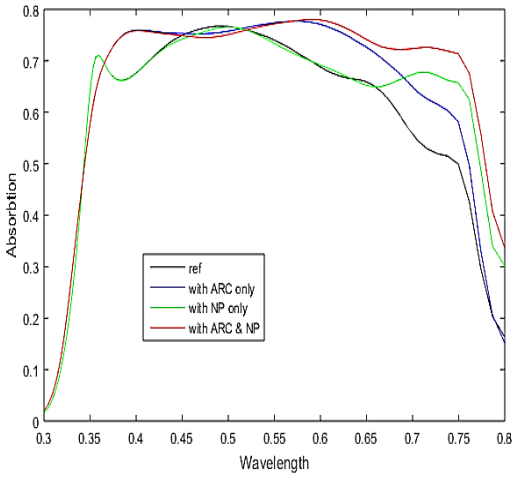

Figure 11. Absorption with different light trapping structures in a 400 nm thick perovskite monolayer.

Table 5. Short-circuit current values and relative gain for different light trapping structures.

Cell structure	J_{sc}(ma/cm^2)	Relative Enhancement of the Jsc (%)
Reference	20.7946	-
With ARC Only	22.4267	7.85
With NP Only	24.0148	15.49
With NP & ARC	25.5591	22.86

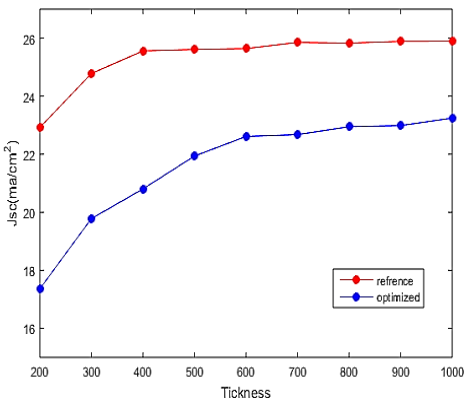

Figure 12. Short circuit current of the reference cell and the cell with light trapping structure for different thicknesses of the perovskite layer.

3.6. Power-voltage and current-voltage characteristics

This part examined electrical modeling utilizing the Device module. The Shockley-Read Hall and surface recombination models were employed for the recombination function, while the drift-diffusion model was utilized for the carrier transport equations. The optical properties of the reference perovskite cell were replicated, and its structure was simulated, with the results documented in Table 6. The carbon-based perovskite cell including the light trapping structure was simulated, resulting in the anticipated enhancement of all electrical parameters. Figure 13 illustrates the power-voltage and current-voltage characteristics of both the reference perovskite cell and the perovskite cell with the trapping structure. This simulation accounts for the light absorbed in the electron and hole transport layers. The negligible change in open-circuit voltage (Voc) and fill factor (FF) despite enhanced JSC can be attributed to two factors: (1) The Shockley-Read-Hall recombination model assumes defect-dominated recombination, which becomes more pronounced at higher carrier densities induced by light trapping. (2) The hybrid structure introduces additional interfaces (e.g., SiO_2/Ag, PMMA/perovskite), potentially creating localized trap states that limit Voc improvement. Future work should incorporate interface passivation strategies to mitigate this trade-off.

Table 6. Parameter values of the reference perovskite cell and the optimized perovskite cell.

Cell structure	Voc	Jsc	FF	η
Reference	0.51584	21.4346	0.806147	8.91342%
Optimized	0.52118	26.5031	0.807701	11.1567%

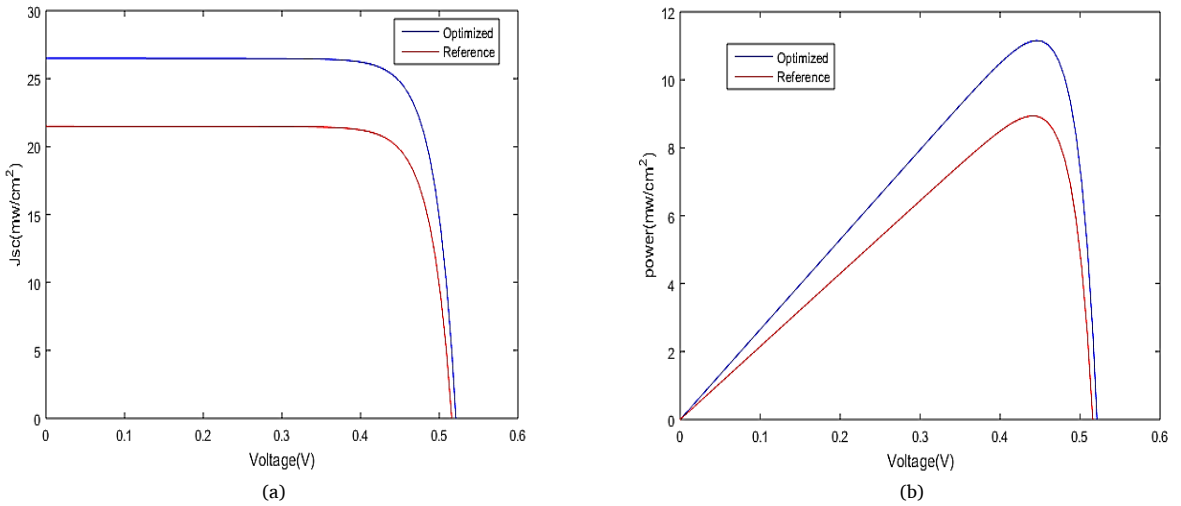

Figure 13. Comparison of the reference perovskite cell and the optimized perovskite cell, a) current-voltage characteristic, b) power-voltage characteristic.

4. Conclusion

This study emphasizes the importance of solar energy and presents various types of solar cells, particularly PSCs. It proposes a hybrid light trapping structure comprising silver core nanoparticles with a silica shell positioned beneath the active perovskite layer, along with a PMMA anti-reflective coating on the front surface, aimed at enhancing the absorption bandwidth in CBPSCs. The enhancement of light absorption can be attained through the meticulous selection of structural parameters, including the radius and period of the silver-silica nanoparticles, along with the thickness of the silica shell and the anti-reflective coating. In comparison to the reference CBPSCs lacking light management, the short-circuit current values with light trapping can be enhanced by 17 to 27%. Additionally, a substantial short-circuit current of 25.264 mA/cm^2 was attained for a 600 nm thick perovskite layer utilizing silver-silica nanoparticles having a radius of 100 nm and a periodicity of 280 nm, along with a 60 nm thick PMMA anti-reflection coating. The efficiency and short-circuit current of the carbon-based perovskite cell with the light trapping structure were enhanced; however, no notable alteration was seen in the open-circuit voltage and fill factor. This technique can serve as a general framework to enhance absorption efficiency while decreasing lead content through the utilization of thinner perovskite in CBPSCs. While the simulation results are promising, practical implementation faces challenges: (1) Precise alignment of Ag/SiO_2 nanoparticles within the perovskite layer requires advanced nanofabrication techniques (e.g., electron-beam lithography), which may increase cost. (2) Long-term stability of PMMA under UV exposure needs experimental validation. (3) Variability in nanoparticle size and distribution could affect performance reproducibility. Future studies should focus on scalable deposition methods (e.g., spin-coating with self-assembled nanoparticles) and accelerated aging tests to evaluate durability.

References

[1] W. S. Yang, B. Park, et al., "Iodide Management in Formamidinium-Lead-Halide–Based Perovskite Layers for Efficient Solar Cells," *Science*, vol. 356, no. 6345, pp. 1376–1379, 2017.

[2] M. Saliba, T. Matsui, et al., "Incorporation of Rubidium Cations into Perovskite Solar Cells Improves Photovoltaic Performance," *Science*, vol. 354, no. 6309, pp. 206-209, 2016.

[3] B. Boroomandnasab, and M. H. Zolfaghari, "Optimization CIGS/CIGS Tandem Solar Cells by Adjusting Layer Thickness Using Silvaco-TCAD," *Journal of Green Energy Research and Innovation*, vol. 1, no. 1, pp. 48–54, 2024.

[4] S. K. Sahoo, B. Manoharan, and N. Sivakumar, "Introduction," *Perovskite Photovoltaics*, pp. 1–24, 2018.

[5] T. Dai, Q. Cao, et al., "Strategies for High-Performance Large-Area Perovskite Solar Cells Toward Commercialization," *Crystals*, vol. 11, no. 3, p. 295, 2021.

[6] F. Ambrosio, J. Wiktor, F. De Angelis, and A. Pasquarello, "Origin of Low Electron–Hole Recombination Rate in Metal Halide Perovskites," *Energy & Environmental Science*, vol. 11, no. 1, pp. 101–105, 2018.

[7] Q. Lin, A. Armin, R. C. R. Nagiri, P. L. Burn, and P. Meredith, "Electro-Optics of Perovskite Solar Cells," *Nature Photonics*, vol. 9, no. 2, pp. 106–112, 2014.

[8] H. Dong, T. Lei, et al., "Plasmonic Enhancement for High Efficient and Stable Perovskite Solar Cells by Employing "hot Spots" Au Nanobipyramids," *Organic Electronics*, vol. 60, pp. 1–8, 2018.

[9] Y. Li, Z. Kou, J. Feng, and H. Sun, "Plasmon-Enhanced Organic and Perovskite Solar Cells with Metal Nanoparticles," *Nanophotonics*, vol. 9, no. 10, pp. 3111–3133, 2020.

[10] W. A. Murray, and W. L. Barnes, "Plasmonic Materials," *Advanced Materials*, vol. 19, no. 22, pp. 3771–3782, 2007.

[11] A. Benayad, D. Diddens, et al., "High-throughput experimentation and computational freeway lanes for accelerated battery electrolyte and interface development research," Advanced Energy Materials, vol. 12, no. 17, p. 2102678, 2022.

[12] E. Raoult, R. Bodeux, et al., "Optical Characterizations and Modelling of Semi-Transparent Perovskite Solar Cells for Tandem Applications," *in 36th European Photovoltaic Solar Energy Conference and Exhibition*, 2019, pp. 757-763.

[13] A. A. Tabrizi, H. Saghaei, M. A. Mehranpour, and M. Jahangiri, "Enhancement of Absorption and Effectiveness of a Perovskite Thin-Film Solar Cell Embedded with Gold Nanospheres," *Plasmonics*, vol. 16, no. 3, pp. 747–760, 2021.

[14] S. Royanian, A. Abdolahzadeh Ziabari, and R. Yousefi, "Efficiency Enhancement of Ultra-Thin CIGS Solar Cells Using Bandgap Grading and Embedding Au Plasmonic Nanoparticles," *Plasmonics*, vol. 15, no. 4, pp. 1173–1182, 2020.

[15] P. R. Pudasaini, and A. A. Ayon, "Nanostructured Thin Film Silicon Solar Cells Efficiency Improvement Using Gold Nanoparticles," *physica status solidi (a)*, vol. 209, no. 8, pp. 1475–1480, 2012.

Declaration of competing interest

The authors declare that they have no known competing financial interests or personal relationships that could have appeared to influence the work reported in this paper. The ethical issues, including plagiarism, informed consent, misconduct, data fabrication and/or falsification, double publication and/or submission, redundancy, have been completely observed by the authors.

Bibliography

Bahareh boroomandnasab was born in 1988, in Dezful, Iran. She received her Bachelor's, Master's, and Ph.D. degrees in Electronics Systems Engineering from Shahid Chamran University of Ahvaz, Ahvaz, Iran in 2011, 2013, and 2019, respectively. She is currently an Assistant Professor in Institute for Higher Education, ACECR, Khuzestan, IRAN. Her research interests include semiconductor device design, simulation and fabrication.

Email: boroomand@acecr.ac.ir

ORCID: 0009-0009-6083-3796

Contribution Statement: Data curation, Formal analysis, Software, Validation, Visualization, Roles/Writing-original draft.

Salem Doreghi is an Electronics Engineer at Karun Oil and Gas Exploitation Company. At work, he repairs all types of power supply and UPS. He was born in 1988. He is from Iran and the city of Ahvaz. He believes that electronic science helps people in all aspects of daily life. He has a master's degree from Institute for Higher Education ACECR Khuzestan.

Email: doraghi.1367@gmail.com

ORCID: 0009-0005-5025-2745

Contribution Statement: Investigation, Software.